Journal of Hazardous Materials 165 (2009) 548–557

Contents lists available at ScienceDirect

Journal of Hazardous Materials

journal homepage: www.elsevier.com/locate/jhazmat

# Particle morphology and mineral structure of heavy metal-contaminated kaolin soil before and after electrokinetic remediation

Nicole Roach[a], Krishna R. Reddy[a], Ashraf Z. Al-Hamdan[b,*]

[a] Department of Civil and Materials Engineering, University of Illinois at Chicago, 842 West Taylor Street, Chicago, IL 60607, USA
[b] Department of Civil and Environmental Engineering, University of Alabama in Huntsville, 301 Sparkman Drive, Huntsville, AL 35899, USA

ARTICLE INFO

*Article history:*
Received 8 May 2008
Received in revised form 7 September 2008
Accepted 6 October 2008
Available online 14 October 2008

*Keywords:*
Electrokinetics
Remediation
Clays
Heavy metals

ABSTRACT

This study aims to characterize the physical distribution of heavy metals in kaolin soil and the chemical and structural changes in kaolinite minerals that result from electrokinetic remediation. Three bench-scale electrokinetic experiments were conducted on kaolin that was spiked with Cr(VI) alone, Ni (II) alone, and a combination of Cr(VI), Ni(II) and Cd(II) under a constant electric potential of 1 VDC/cm for a total duration of 4 days. Transmission electron microscopy (TEM), energy dispersive X-ray spectroscopy (EDX), and X-ray diffraction (XRD) analyses were performed on the soil samples before and after electrokinetic remediation. Results showed that the heavy metal contaminant distribution in the soil samples was not observable using TEM and EDX. EDX detected nickel and chromium on some kaolinite particles and titanium-rich, high-contrast particles, but no separate phases containing the metal contaminants were detected. Small amounts of heavy metal contaminants that were detected by EDX in the absence of a visible phase suggest that ions are adsorbed to kaolinite particle surfaces as a thin coating. There was also no clear correlation between semiquantitative analysis of EDX spectra and measured total metal concentrations, which may be attributed to low heavy metal concentrations and small size of samples used. X-ray diffraction analyses were aimed to detect any structural changes in kaolinite minerals resulting from EK. The diffraction patterns showed a decrease in peak height with decreasing soil pH value, which indicates possible dissolution of kaolinite minerals during electrokinetic remediation. Overall this study showed that the changes in particle morphology were found to be insignificant, but a relationship was found between the crystallinity of kaolin and the pH changes induced by the applied electric potential.


## 1. Introduction

In the United States, about 500,000 potentially contaminated sites have been reported to the state and federal authorities, and of these, over 217,000 require urgent remediation to protect public health and the environment [1]. The conventional remediation technologies, such as bioremediation, soil flushing, and thermal desorption, have proven to be expensive or ineffective when applied to low-permeability soils. The electrokinetic (EK) soil remediation method has received the attention of environmental professionals recently because it has the potential to remove pollutants from low permeability soils. Electrokinetic remediation involves installation of electrodes into multiple wells within a contaminated zone, followed by the application of a low electric potential. Ideally, the contaminants migrate toward the electrodes due to different transport mechanisms, and when the contaminants reach the wells, the contaminant-laden liquids are extracted and treated. Although its implementation is simple, the geochemical processes that occur within soil during electrokinetic remediation are complex, and are dependent on system variables such as soil type, contaminant type, treatment time, electrolyte solution, and applied voltage.

Electrokinetic remediation of heavy metals in soils has been investigated at the University of Illinois at Chicago [2–6]. These studies demonstrated that in low buffering soils such as kaolin with water as the electrolyte solution, targeted metal cations such as nickel and cadmium migrate toward the cathode and are immobilized before they reach the cathode. Anionic contaminants such as hexavalent chromium migrate toward the anode and are then immobilized within the soil closer to the anode. Overall contaminant removal from the soil was found to be very low. Sequential chemical extraction methods and geochemical modeling were used to obtain a better understanding of the processes hindering the contaminant removal. The results suggested that the cationic metal contaminants were immobilized by adsorption and precipitation

* Corresponding author. Tel.: +1 256 824 6117; fax: +1 256 824 6724.
*E-mail addresses:* alhamdan@eng.uah.edu, ashrafalhamdan@gmail.com (A.Z. Al-Hamdan).

0304-3894/$ – see front matter © 2008 Elsevier B.V. All rights reserved.
doi:10.1016/j.jhazmat.2008.10.022

reactions, while the anionic contaminants were immobilized by adsorption reactions, and also possibly by reduction reactions. To date, however, a detailed investigation of physical distribution of contaminants and changes in soil minerals before and after electrokinetic remediation has not been performed. Information acquired from such an investigation can be immensely valuable for a better understanding of the geochemical processes occurring within the soil during EK and for developing rational approaches to optimize contaminant mobility and removal.

The objective of this study was to investigate the physical distribution of heavy metals in kaolin and the chemical and structural changes in kaolinite minerals that result from electrokinetic remediation. Transmission electron microscopy (TEM) and energy dispersive X-ray spectroscopy (EDX) analyses of kaolin soil samples spiked with heavy metals were performed before and after electrokinetic remediation. In addition, X-ray diffraction (XRD) analyses of metal-spiked kaolin soil were performed before and after electrokinetic remediation.

## 2. Background

Electrokinetic remediation involves the application of a direct current to low-permeability soils to induce flow of water, ions and/or particles toward electrode wells where they can be removed. This method is attractive for the remediation of soils with high clay mineral content because the processes that govern electrokinetic contaminant transport are not as easily hindered by low hydraulic conductivity. The two main mechanisms that govern electrokinetic contaminant transport are electroosmosis and electromigration. Electroosmosis is simply the flow of water through a charged soil medium under the influence of an electric field [7]. Electromigration involves the movement of ions under electrostatic attraction toward an anode or cathode, where the direction of travel depends on the charge of the ion. The extent of electroosmosis and electromigration processes is highly dependent on physicochemical processes that take place in the soil and at the electrodes [8].

In low permeability soils with a surface charge, electric conduction involves the one-way movement of counter-ions, which are ions with a charge that is opposite the mineral surface charge. These ions carry waters of hydration and bulk water with them, generating electroosmotic flow. The idea is for dissolved contamination to be swept away with the flow of water and to also migrate through the water, ultimately reaching electrodes where it can easily be removed. In order for electroosmosis and electromigration to effectively move metal contaminants, the metal ions must first be in solution.

During the electrokinetic decontamination process, electrolysis reactions take place at the anode and the cathode:

$$H_2O \rightarrow 2H^+ + \tfrac{1}{2}O_2(g) + 2e^-(\text{anode}) \quad (1)$$

$$2H_2O + 2e^- \rightarrow H_2(g) + 2OH^-(\text{cathode}) \quad (2)$$

These reactions produce hydrogen ions ($H^+$) at the anode and hydroxyl ($OH^-$) ions at the cathode, creating acidic and alkaline conditions, respectively. Generally, the resulting acid front migrates toward the cathode under the influence of bulk water flow and the high ionic mobility of $H^+$. The acid front can free adsorbed metal cations from clay mineral surfaces and also dissolve heavy metal precipitates like carbonates and hydroxides that are otherwise immobile. Dissolved cations are then free to move through the soil and ideally to the cathode reservoir where they can be removed. The $OH^-$ ions that are produced near the cathode tend to join with approaching metal cations to form metal precipitates, thereby immobilizing the metals before they reach the cathode. Enhancements have been added to the cathode, such as acetic, citric, and lactic acids, in efforts to lower the cathode pH and prevent metal cation precipitation [4,9–11].

EK processes also depend on contaminant speciation. For example, hexavalent chromium exists in anionic complex ($Cr_2O_7^{2-}$, $CrO_4^{2-}$ or $HCrO_2$ depending on Eh-pH conditions), higher pH (alkaline) conditions favor it to exist in solution [12]. If low pH conditions exist, buffering agents are added to maintain alkaline conditions and enhance Cr(VI) mobility and removal [13,14]. Cosolvents [15–18], oxidation agents [19,20] and reducing agents [21] have also been used to control these secondary reactions when treating hydrophobic organic contaminants as well as metal cations. Other reactions that contribute to the complexity of the electrokinetic soil remediation process are desiccation due to heat generation at electrodes, gas generation at electrodes from electrolysis, oxidation and reduction of contaminants and other soil constituents, soil fabric change, mineral dissolution and precipitation of minerals and oxides [22].

The electrokinetic soil remediation method (EK) is a complicated process that is highly dependent on soil pore fluid chemistry, the mineralogical composition of the soil, and contaminant type and speciation. Variations in pore fluid chemistry can affect the speciation and distribution of a contaminant through redox reactions, precipitation/dissolution or adsorption/desorption processes. For example, nickel may be adsorbed to the surface of soil, but introducing acidic pore fluid can desorb nickel ion and make it migrate through the soil towards the cathode under applied electric potential. Pore fluid chemistry can also affect soil mineralogy by causing soil minerals to dissolve or metal precipitates to form. For example, some kaolinite platelets may dissolve during EK as a result of pH changes within the pore fluid, namely at pH values above 9 and below 4 [23,24]. Soil mineralogy can, in turn, affect pore fluid chemistry through the release of new ionic species [25]. Contaminant type or speciation can affect the mineralogical composition of a soil through complexation reactions. For example, a metal contaminant in cationic form may form an inner-sphere complex between two opposing tetrahedral layers of an expandable clay like montmorillonite. Once the cation has complexed with the clay, it may not be the same species. Despite many studies, uncertainty exists concerning the physicochemical processes that take place during EK; therefore, a better understanding of these processes is needed to optimize contaminant mobility and removal during electrokinetic remediation.

A number of research studies have been performed at the University of Illinois at Chicago (UIC) to understand the transport processes and geochemical reactions that affect the removal of heavy metals from low permeability soils. Reddy et al. [2] investigated kaolin soil spiked with Cr(VI) alone, Ni(II) alone, and a combination of Cr(VI), Ni(II) and Cd(II). Al-Hamdan [26] generated a series of geochemical models by utilizing concentration and pH data from the tests that were performed by Reddy et al. [2]. Kaolin is a common soil medium used in bench-scale EK experiments. It is a low permeability soil that is composed almost purely of kaolinite clay minerals, with a few additional trace substances. Kaolin is fairly non-reactive compared to other clays, and because EK remediation processes are already complicated, its use as an experimental soil medium helps to reduce the number of variables associated with more reactive clays or soils with more complex mineralogical compositions. The kaolin used in all experiments at UIC was obtained from EM science, CAS # 1332-58-9. The clean kaolin soil was examined using transmission electron microscopy and observed grains were hexagonal in shape, often displaying a mottled appearance at the particle surface. The dominant mineral in the kaolin soil, kaolinite $Al_2Si_2O_5(OH)_4$, occurs in hydrothermal, residual and sedimentary deposits, and is formed under relatively low temperatures and pressures [27]. The most common parent minerals from which

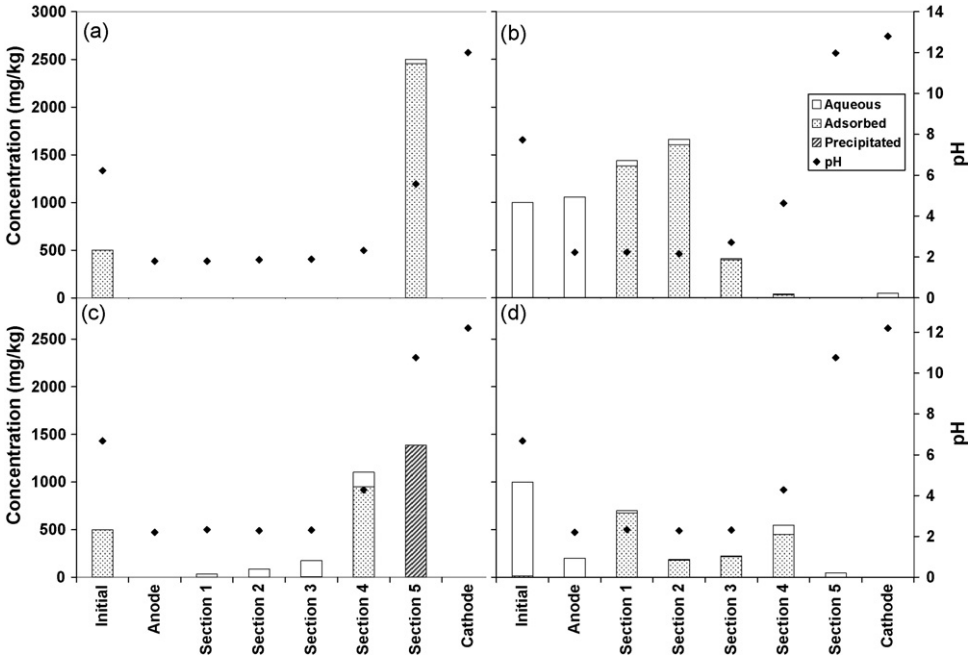


**Fig. 1.** Heavy metal concentrations and pH of soil after electrokinetic remediation: (a) Ni only test, (b) Cr only test, (c) mixed contaminants (Cr, Ni and Cd) test: Ni concentration, and (d) mixed contaminants (Cr, Ni and Cd) test: Cr concentration. (The metal concentrations in the anode and cathode reservoirs are converted from mg/L to mg/kg for mass balance purposes.)

kaolinite forms are feldspars and muscovite, so granites, which contain abundant feldspar and mica, weather readily to kaolinite and quartz under conditions that are favorable to its formation such as high rainfall, rapid drainage, temperate to tropical climate, a low water table, and adequate ground water movement to leach the soluble components [27].

The initial and final metal concentrations and soil pH determined from previous EK tests performed by Reddy et al. [2] are illustrated in Fig. 1. It should be mentioned that soil samples used were cylindrical in shape with diameter of 6.2 cm and length of 19.1 cm. After electrokinetic testing, the soil sample was extruded and divided into five equal sections. The measured metal concentrations for these sections were plotted against normalized distance (distance from the anode divided by the total length of the sample) from the anode. Sections are designated as Sections 1–5 with the Section 1 being the closest to the anode and Section 5 being the closest to the cathode. For the test where nickel was the only contaminant, almost all of the positively charged nickel ions ($Ni^{2+}$) migrated to Section 5, where they were immobilized due to precipitation under the high pH conditions [2]. For the test where hexavalent chromium was the only initial contaminant, the two sections near the anode contained about 65% of the total chromium, which may have been due to migration of hexavalent chromium toward the anode and then adsorption onto clay particle surfaces within the low pH environment [2]. Finally, for the test containing multiple contaminants, migration of metals was inhibited by the presence of the other contaminants [2].

Geochemical modeling was performed to assess how the metal contaminants were bound to the soil after electrokinetic remediation [28–30]. This information is useful because it facilitates an understanding of the processes that take place during electrokinetic remediation. MINEQL+, a chemical equilibrium computer program model developed by Schecher and McAvoy [31], was used to determine the forms of the contaminants in the soil after electrokinetic remediation (i.e., aqueous, adsorbed, and precipitated). The required input data for the modeling includes major chemical components present in the system, the total concentrations of these components, and surface complexation reactions between the components and the solid. Nickel distribution and speciation in kaolin for the two tests that contained nickel is shown in Fig. 1. The pH decreased with the application of electric potential and brought the adsorbed $Ni^{2+}$ in Sections 1–4 into aqueous phase. The ions were then migrated to Section 5, where the pH was high, and were subsequently immobilized through adsorption and precipitation. The typical results of the geochemical modeling for chromium are shown in Fig. 1. In the electrokinetic test with only Cr(VI), about 60% of the total chromium was accumulated in adsorbed form in Sections 1 and 2, closest to the anode. The area where the most chromium existed in adsorbed form may represent the location where the acid front and the net accumulated chromium anions met.

Although the practical implementation of electrokinetic remediation technology is simple, the geochemical processes associated with it are complex and not completely understood. Previous research on electrokinetics at UIC has helped to understand the effects of different contaminant types, single and multiple contaminants, different soil mineralogical compositions and different pore-fluid chemistries on electrokinetic remediation. Geochemical characterization [2] and modeling [28–30] have implied that adsorption and precipitation are the two dominant processes associated with immobilization of metal contaminants in kaolin soil during electrokinetic remediation. This paper presents complementary study which involves the use of TEM, EDX and XRD to provide a better understanding of contaminant distribution and changes in soil minerals. This knowledge can help environmental professionals to optimize contaminant mobility and removal during electrokinetic remediation.

## 3. Research methodology

Three electrokinetic experiments conducted at UIC were selected for this study: kaolin that was spiked with Cr(VI) alone, Ni(II) alone, and a combination of Cr(VI), Ni(II) and Cd(II). These tests were conducted with a constant electric potential of 1 VDC/cm

for a total duration of 4 days. Kaolin soil samples before and after electrokinetic remediation were analyzed with TEM and EDX detector. To obtain information on the migration of contaminants and their distribution from the anode to the cathode following electrokinetic remediation, each of five sections was analyzed. It was aimed to find and note the approximate location (Sections 1–5) of any changes in heavy metal phase, or changes in kaolinite platelets, resulting from EK treatment, that are observable with a transmission electron microscope and EDX detector. These changes may include the precipitation of separate heavy metal phases, or alterations in clay particle morphology that resulted from reactions with contaminants such as contaminant adsorption or precipitation onto clay particle surfaces. These changes may also include dissolution of kaolinite grains, which may be observable through visible loss of the hexagonal kaolinite structure. Results of the TEM/EDX analysis were compared to geochemical modeling and measured metal concentrations for these EK tests. X-ray diffraction analysis was also performed for all five sections of each test to investigate whether any structural changes occurred in kaolin during electrokinetic remediation.

### 3.1. TEM and EDX analysis

TEM images were collected using a JEOL JEM-3010 Transmission Electron Microscope with a digital camera and Digital Micrograph, Version 3.3.1 software. Semiquantitative chemical analysis was done using Noran Instruments EDX detector with a Vantage digital acquisition engine and the Vista Version 2.2 software. In preparation for analysis with the TEM, each soil sample was air dried, crushed and homogenized. A small amount of sample was dusted over a holey-carbon, 200-mesh copper TEM grid of about 3-mm in diameter. For each sample grid (one or two were prepared for each section), a search for points of interest was done and images and EDX patterns were collected from those areas. A point of interest is defined as any kaolinite particle that appears abnormal, or any other particle that is visually different from the easily identifiable, hexagonally shaped kaolinite particle. Sections containing the most metal contamination were analyzed in greater detail.

### 3.2. X-ray diffraction analysis

X-ray diffraction analyses were done using a Siemens D5000 powder diffractometer with Jade 5.0 software. Other materials used include an aluminum powder holder, which is an aluminum plate with a quartz window where the sample is actually placed. The quartz is oriented 6° off center of the *c*-axis to eliminate the possibility of diffraction from the slide itself. Among other needed materials were small quartz slides for smear mounts, a mortar and pestle, a razor blade, and a dropper bottle containing deionized water. A diffraction pattern was acquired for initial spiked soil and each soil section from three EK tests. The samples for the test with multiple heavy metals were prepared as random backfill mounts. Preparation of a random backfill powder mount included first the gentle crushing of the sample into a powder, taking care not to grind. A glass slide was then taped onto the front of the powder holder and the sample loaded from the back, gently pressing it into the cavity and avoiding any shearing motion. This was done to avoid preferred orientation of grains. The mount was flipped back over and the glass slide carefully removed, revealing the surface that would be exposed to the X-ray beam. The soil samples from the other two tests containing chromium only and nickel only were mounted using the smear technique. Smear mounts were prepared by gently crushing the sample into a powder using a mortar and pestle. A small amount of sample was mixed with deionized water and the mixture was dropped onto a slide and allowed to dry.

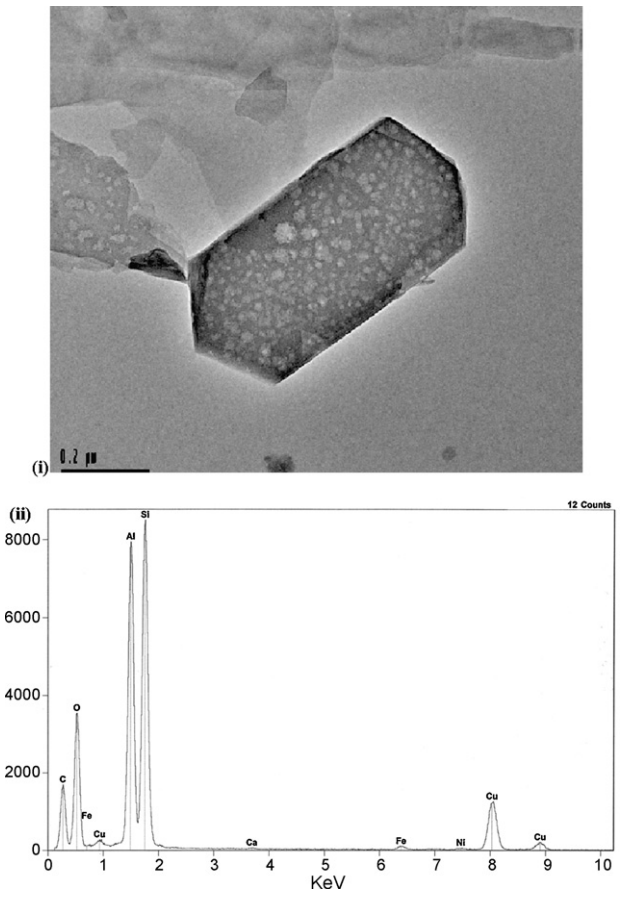


**Fig. 2.** EK test with Ni only, initial spiked soil sample: (i) TEM image, (ii) EDX spectrum.

This method of sample preparation does not produce a random orientation of grains, but a preferred orientation limiting observable changes to those that take place along the c-axis; therefore, only 0 0 l peaks were examined.

## 4. Results and discussion

### 4.1. TEM and EDX results

The TEM and EDX data for samples of initial metal-spiked soil and Sections 1–5 of each EK test (Section 1 near the anode and Section 5 near the cathode) were obtained [32], but only the main results are presented and discussed for each test.

#### 4.1.1. Nickel only test

A group of particles from within the initial nickel-spiked sample of kaolinite, before electrokinetic remediation, is shown in Fig. 2. The mottled surficial appearance on the kaolinite grain surface, along with the worn-looking edges, should be noted. The EDX spectrum (Fig. 2) shows that a small amount of nickel is present, about 0.01 wt%. Also, 0.02 wt% iron and 0.02 wt% calcium were detected from this group of particles. The iron and calcium, along with any other elements with excluding added contaminants, are natural constituents of the kaolin clay that was used for this study.

A TEM image of particles from Section 1 (nearest to the anode) showed mottled appearance on the kaolinite grain surfaces similar to what was observed in the initial sample. The EDX pattern showed 0.02 wt% iron. The black deposit on the right side of the image, which was also analyzed with EDX, is composed mostly of

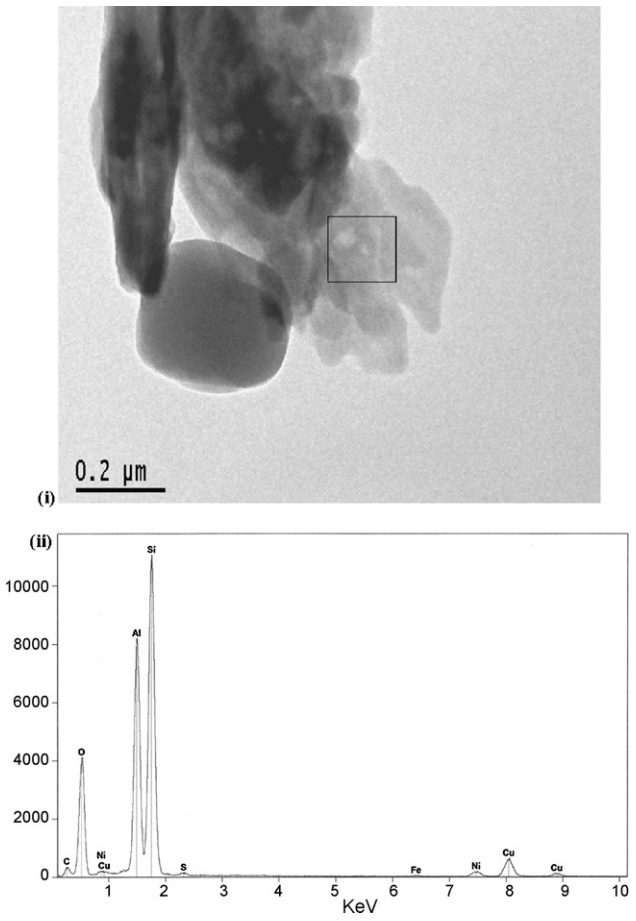


**Fig. 3.** EK test with Ni only, Section 5: (i) TEM image, (ii) EDX spectrum.

iron as well. No nickel was detected in this sample. Similar to Section 1, the TEM image for Section 2 visually resembled the initial soil, except for the lack of visually recognizable surface texture. The mottled appearance was not as apparent in this image. The EDX spectrum showed no signs of nickel and iron was detected in the amount of 0.03 wt%. A TEM image from Section 3 showed kaolinite grains that resemble the samples of Sections 1 and 2. There were no signs of nickel within this image. The EDX showed the presence of traces of iron and the presence of silicon, aluminum and oxygen. In the TEM image taken from a sample of Section 4, there was an amorphous looking area, and the EDX pattern showed that the kaolin soil was siliceous material (composed of mostly silicon, oxygen and aluminum), but the TEM image suggested that it has lost its general hexagonal structure. This observation indicates possible dissolution of the kaolinite during electrokinetic remediation. Eykholt [33] reported that kaolinite dissolves more readily in highly basic or highly acidic conditions, more so in basic conditions; but the soil pH of 4 in this section does not support the occurrence of significant mineral dissolution. The TEM image for Section 5 is shown in Fig. 3 and it indicates broken down and without an ordered structure, and the soil pH is high in this section (about 10.8) so this particle is a possible indicator of mineral dissolution. As mentioned previously, the majority of nickel migrated to Section 5 of the soil (near the cathode), where it was immobilized due to the abrupt increase in soil pH [2]. Some nickel was detected by EDX analysis (Fig. 3), but only 0.02 wt%. Although 0.02% is double the amount that was found in the initial sample (0.01%), the concentration of nickel in the initial sample was not 50%, but 80% less than what was found in Section 5.

*4.1.2. Chromium only test*

A group of kaolinite particles from the initial kaolinite sample, before electrokinetic remediation, spiked with hexavalent chromium, appear in Fig. 4. Most of the particles appear to be well crystallized. The EDX pattern (Fig. 4) shows a trace of chromium, about 0.01 wt%. About 0.02 wt% iron is detected in this section as well.

The TEM images from Section 1 revealed that soil particles appear normal, but some rough edges were observed. According to Reddy et al. [2], the initial sample has a chromium concentration that is about 20% less than the chromium concentration in Section 1. However, no chromium was detected in this sample. The reason for this could be that chromium distribution within the section was not uniform, and if chromium was present within the particles selected, it was below detectable levels. Based on the chemical concentrations reported by Chinthamreddy [34], the largest amount of chromium resides in soil Section 2. TEM images and EDX analysis results shown in Fig. 5 indicate the presence of some chromium in this section, about 0.1 wt%, but there are no visible signs of anything attached to the soil. The particle section from which EDX spectrum (within the white box) is acquired has no smaller particles attached to it or next to it (Fig. 5). This small area is not hexagonal in shape, but silicon and aluminum are still far more abundant than the chromium (17.94 and 22.1 wt%, respectively) and there do not appear to be any other particles beneath it, so this is clearly not a section that is dominated by chromium, but rather, may have some chromium adsorbed to its surface. The value of 0.1 wt% for Section 2 is an order of magnitude greater than the percentage of chromium detected in the initial sample (Fig. 5). The TEM

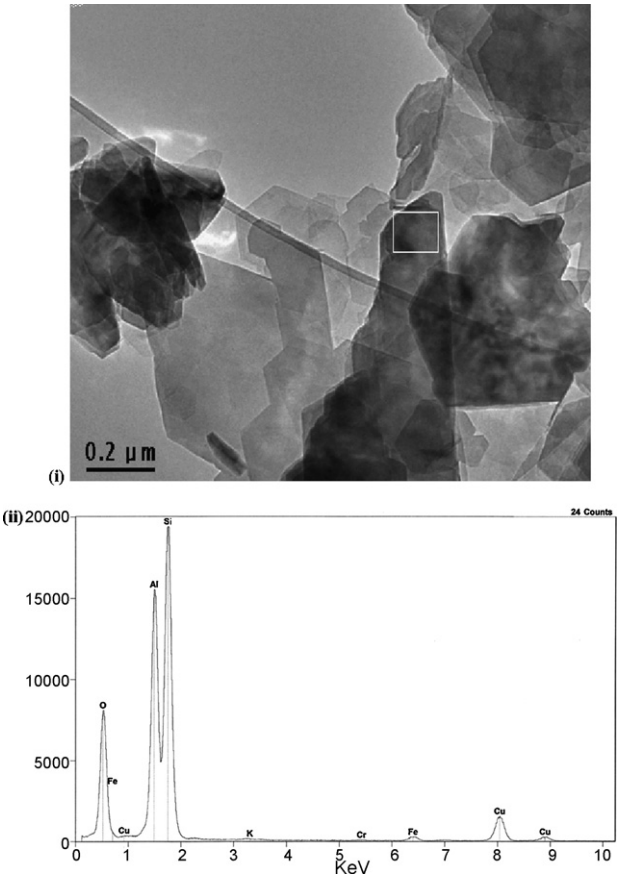


**Fig. 4.** EK test with Cr only, initial spiked soil sample: (i) TEM image, (ii) EDX spectrum.

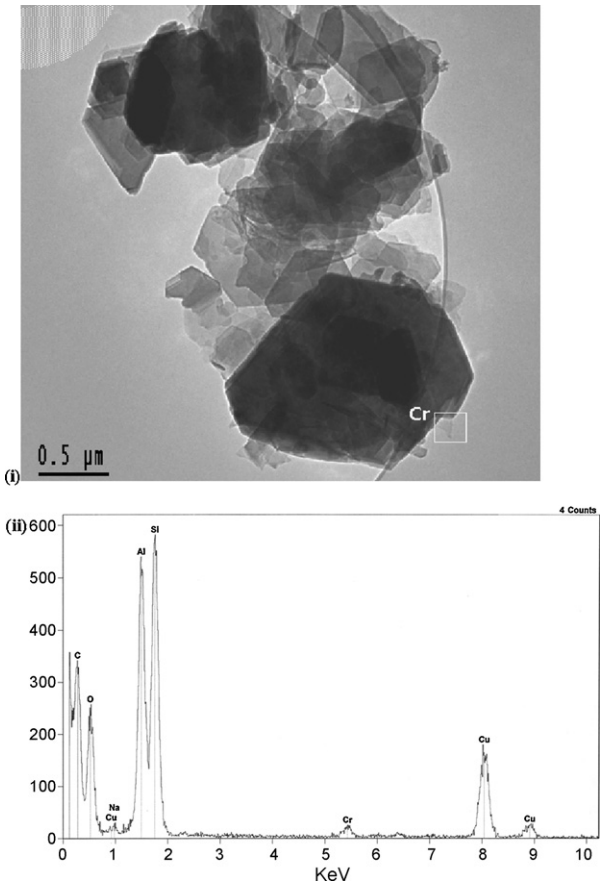


**Fig. 5.** EK test with Cr only, Section 2: (i) TEM image, (ii) EDX spectrum.

images of Section 3 showed the mottled surface appearance that is periodically visible in this kaolinite. Based on the EDX analysis, no chromium was detected in this section. This particle, however, contains a little more iron than what was observed in Sections 1 and 2 (0.08 wt%), but is still mostly composed of silicon and aluminum. About 0.33 wt% potassium was detected as well. A TEM image of Section 4 showed the same mottled appearance as for Section 3. Chromium was not detected with EDX analysis, but this is not surprising because Reddy et al. [2] results show a chromium concentration of only 47 mg/kg in this section. The higher-contrast particle contains about 1.16 wt% calcium and 1.42 wt% phosphorous, according to the EDX pattern. The EDX spectrum shows a high silica and aluminum content as well, but the TEM image shows that this particle overlaps a larger group of kaolinite grains, so it is difficult to determine whether this particle is silica rich. The TEM image from Section 5 showed several high-contrast particles but no chromium was detected here. Reddy et al. [2] reports a concentration of zero for chromium in this section. Potassium and iron appear in the EDX spectrum at 1.09 and 0.12 wt%, respectively.

### *4.1.3. Combined chromium, cadmium and nickel test*

There was a significant amount of nickel and cadmium migration, with relatively higher concentrations of nickel and cadmium detected in soil Sections 4 and 5. Nickel and chromium were both detected in this section with EDX; however, no cadmium was detected. Unlike the chromium test and the nickel test, high-contrast amorphous deposits appear frequently in both the initial sample (pre-EK) and post-EK soil sections for this multiple contaminant experiment. This could be the result of heterogeneity within the natural kaolin deposit from which the clay was collected. In an image taken from the initial sample, one of these high-contrast deposits is marked "a" (Fig. 6). The EDX spectrum corresponding to it (Fig. 6) indicates a significant amount of titanium, about 4.85 wt%. There is also 0.01 wt% of iron in the EDX spectrum as well. Area b, adjacent to this titanium rich particle (EDX not shown) has an EDX spectrum with only oxygen, silicon and aluminum.

A mottled surface appearance was observed in the TEM image for Section 1 (Fig. 7). Chromium, titanium and iron were observed at 0.14, 5.4 and 0.09 wt%. The grains in an image taken from Section 2 appeared well crystallized, with sharp hexagonal edges, and the EDX spectrum showed about 8.08 wt% titanium, 0.50 wt% iron and 0.29 wt% chromium (double the amount found in Section 1). From these results, chromium detection seems stronger when it is associated with titanium. Fig. 8 shows TEM and EDX results for Section 3. The titanium rich particles were observed to contain 0.63 wt% (much less than in the other similar-looking particles). The lower percentage of Ti may be due to the visible overlying and underlying kaolinite grains, which contribute significant silicon, aluminum and oxygen. It should be noted that the electron beam is penetrating the sample and detecting all materials above and below. About 0.03 wt% of chromium was detected in this section as well. There was no chromium detected in the area encompassed by the second white box, near the particle edge (Fig. 8) which again implies that the chromium ions are attracted to the titanium particles. The image taken from Section 4 showed another group of titanium-rich particles that appear to be well-crystallized kaolinite grains. Ti appeared in the EDX spectrum and accounted for about 4.79 wt% of this area, while 0.05 wt% of chromium was found. A trace of iron,

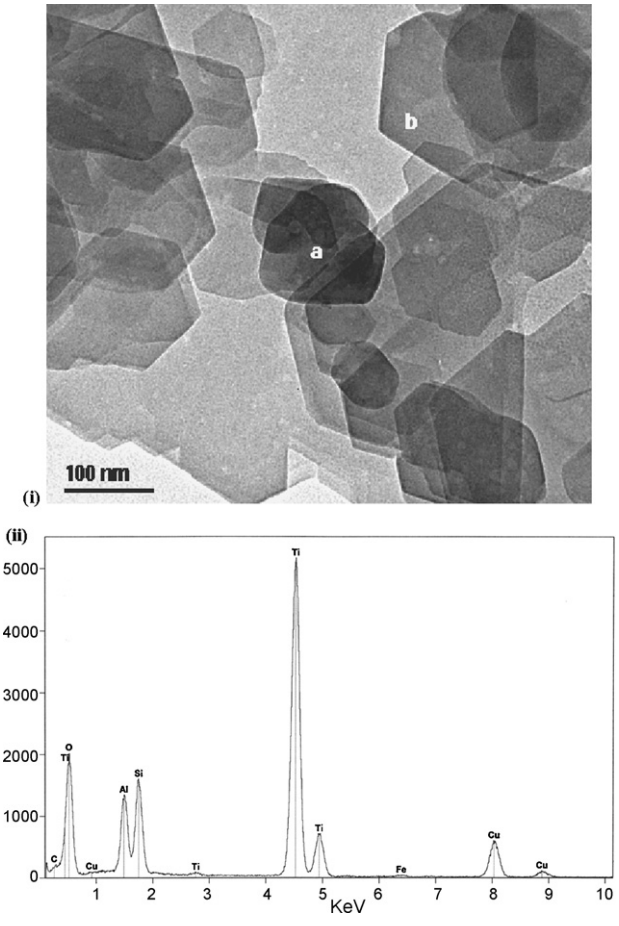


**Fig. 6.** EK test with Cr, Ni and Cd, initial spiked soil sample: (i) TEM image, (ii) EDX spectrum.

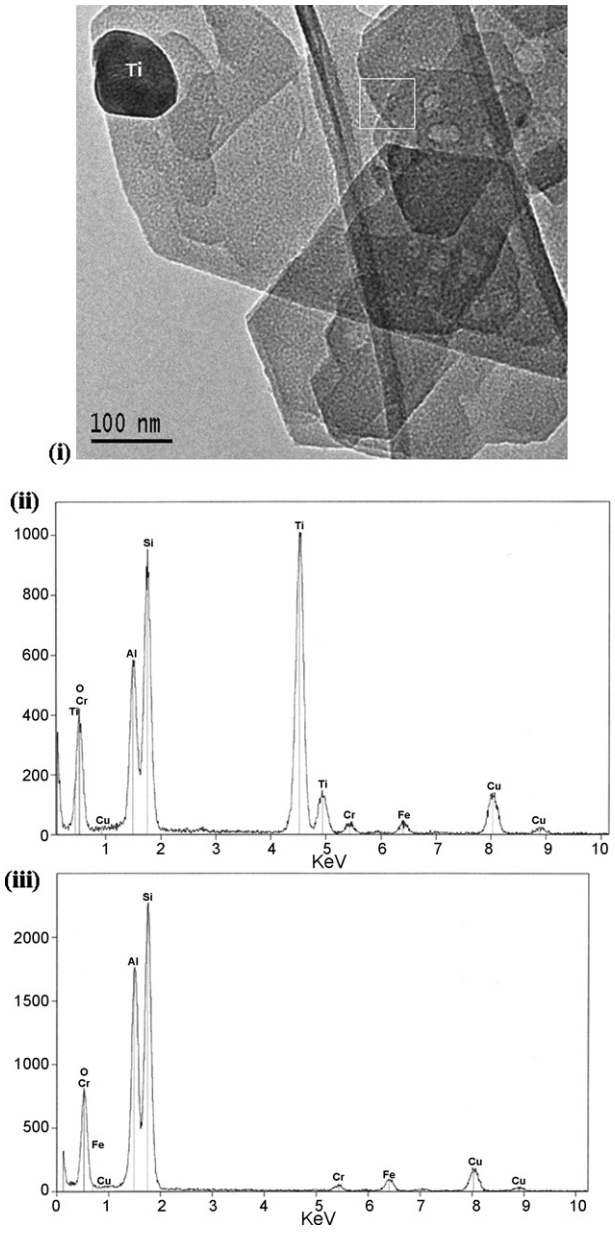


**Fig. 7.** EK test with Cr, Ni and Cd, Section 1: (i) TEM image, (ii) EDX spectrum of Ti particle, (iii) EDX spectrum for area within box.

0.03 wt%, was also present. No nickel or cadmium were detected here or in any of the spectra collected from this test, even though Reddy et al. [2] results indicate a high concentration of nickel and cadmium within this section. Fig. 9 shows TEM and EDX results for Section 5 and it showed particles that are rich in titanium (Section a), but no chromium was detected based on EDX analysis. This is not surprising because Section 5 is the section that shows the lowest concentration of chromium according to Reddy et al. [2]. Contrary to the high measured concentrations of these metals by Reddy et al. [2], nickel and cadmium were not detected in this sample with EDX analysis. The area marked "b" contained no metal impurities.

### *4.1.4. Discussion*

Geochemical modeling results [28–30] indicated that wherever the heavy metals existed, either they existed in the dissolved phase or they were adsorbed to the soil surface. The only exception was in Section 5 of the combined chromium, cadmium and nickel test, where the model predicted that nickel would exist in the precipitate form. It should be noted that the soil samples used for TEM and EDX analysis were dry, so there were no longer any metals existing in the dissolved phase. According to the modeling, the only section where precipitates should have been observed was the Section 5 of the multiple contaminant (Cr, Cd, and Ni) test. Within this section, nickel is the only metal that was predicted to exist in precipitate form because of characteristics specific to the element, and the high pH conditions in that section (soil pH = about 10.8). However, nickel precipitates were not detected within any of the TEM images. In order to further investigate the Section 5 of the Cr, Cd and Ni test, an additional and carefully prepared TEM grid containing soil from this section was examined with the assistance of a well-trained microscopist at a much higher magnification (up to 500,000×). No traces of nickel were found in the precipitate form. There were no visible signs of metal contamination in any initial or post-EK samples, yet small amounts of metal contamination were still detected with EDX analysis. There were simply thin ionic coatings on the clay (adsorption) that would explain the lack of visible phases in all other sections, but would not explain the absence of

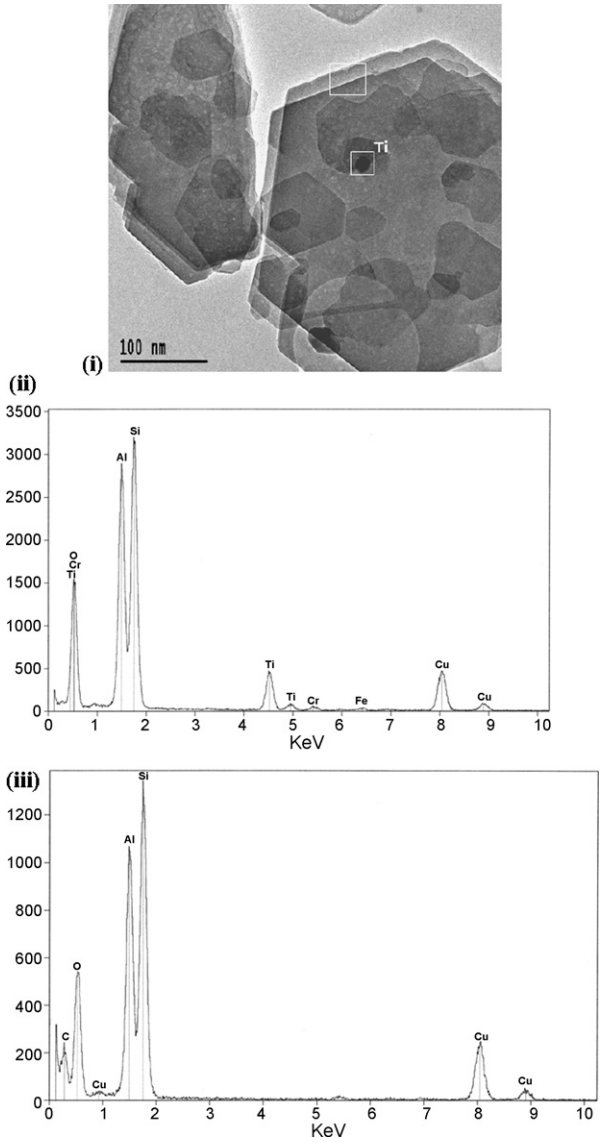


**Fig. 8.** EK test with Cr, Cd and Ni, Section 3: (i) TEM image, (ii) EDX spectrum of Ti-rich particle, (iii) EDX spectrum of area in box.

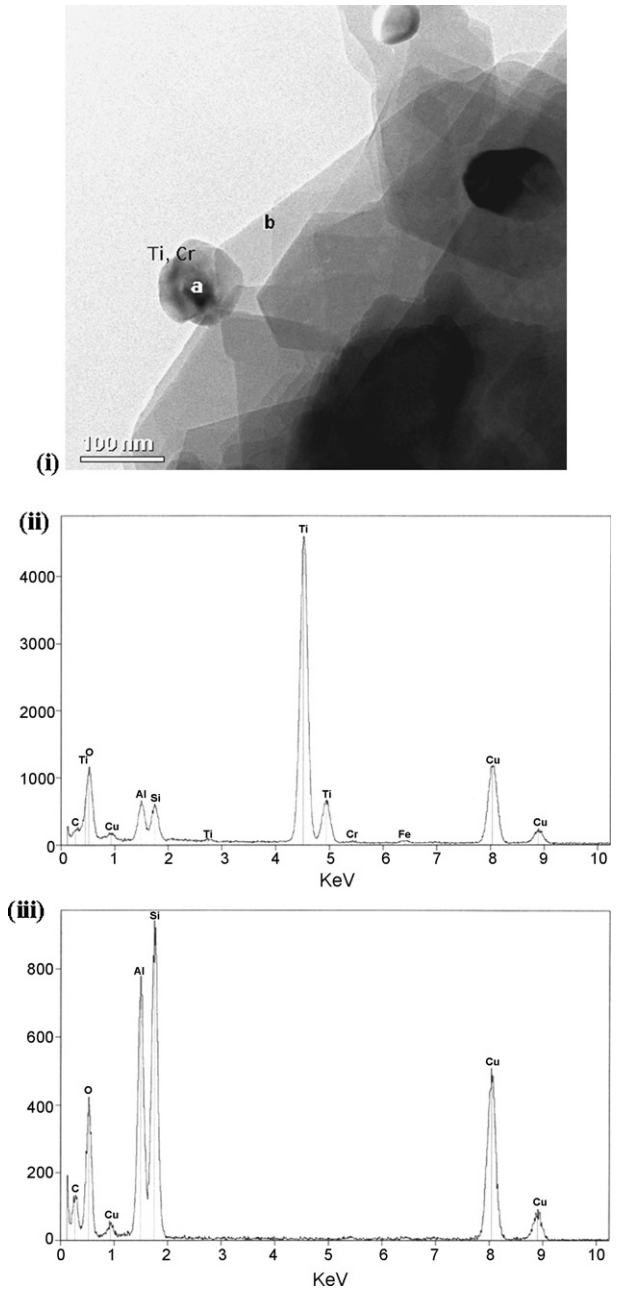


**Fig. 9.** EK test with Cr, Cd and Ni, Section 5: (i) TEM image, (ii) EDX spectrum of area a, (iii) EDX spectrum of area b.

visible nickel precipitates in Section 5 of the multiple contaminant test.

Overall, based on the analysis of soil samples from three different electrokinetic tests spiked with Ni alone, Cr alone, or a combination of Cr, Ni and Cd, the following observations were made. As stated earlier, the mottled surface appearance is not a result of particle damage due to electrokinetics because the same features were found in the spiked kaolinite samples before EK. It is also certain that this is not heavy metal contamination, because the same mottled surface was observed in clean kaolinite samples. Therefore, heavy metal contaminant distribution in these specific soils was not observable using TEM and EDX. There was EDX detection of nickel and chromium on some kaolinite particles and most high-contrast titanium-rich particles, but there was no detection of any separate Ni, Cd or Cr phase. It is possible that detected Ni and Cr are adsorbed onto kaolinite particle surfaces as a thin coating, which might explain their invisibility. This notion is consistent with geochemical models generated by Al-Hamdan and Reddy [28,30], with the exception of the conclusion for Section 5 of the multiple metal test. For that section, the model predicted the existence of nickel in precipitate form, and none was found during this study. Non-detection of precipitated nickel could be the result of low metal concentrations, small sample size, and lack of a sample that represents the entire soil section.

There was also no clear correlation between semiquantitative analysis of EDX spectra and the measured total concentrations. Either the EDX detector was not sensitive to the concentrations in which these metals were present (concentrations below 2750 mg/kg) or the soil samples chosen in each case were not representative of the entire soil section. Both of these reasons are likely. A single clay particle or cluster of clay particles is examined at a time, but they may not represent the soil section as a whole. Had metal concentrations been higher, however, then evidence of the

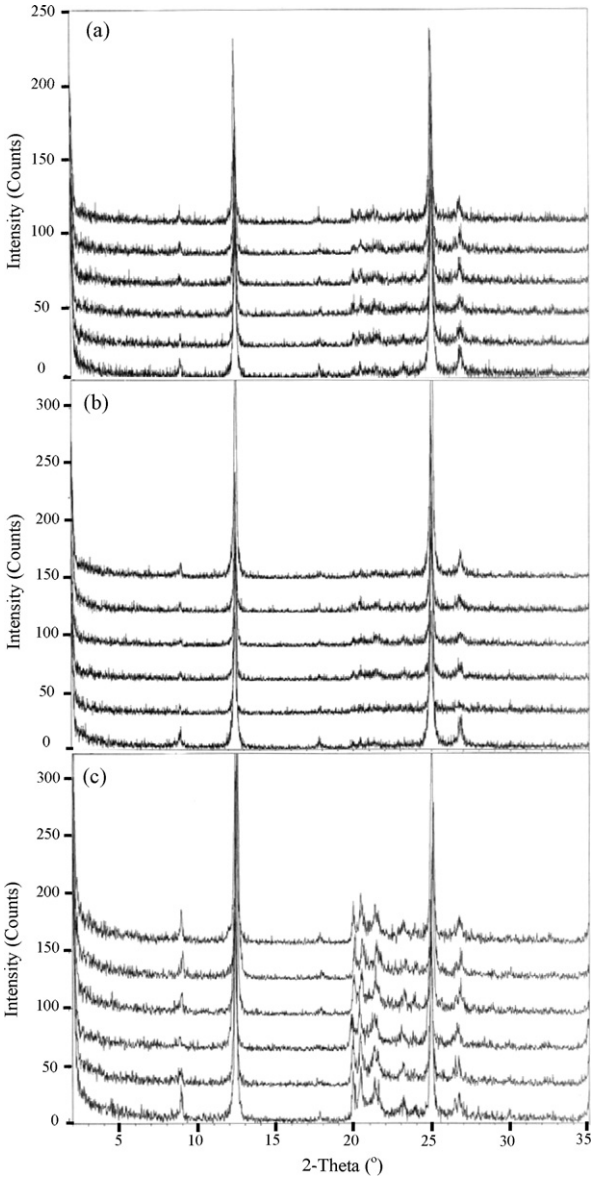


**Fig. 10.** X-ray diffraction pattern of kaolin (a) Ni only test, (b) Cr only test, and (c) mixed contaminants (Cr, Ni and Cd) test. (The pattern at the bottom of each figure is the initial sample; above it is Section 1 of the EK test, then Sections 2–5, respectively.)

contamination could have been more abundant, therefore more frequently observed and more easily studied. There may have been visible evidence of kaolinite dissolution in Section 4 of the nickel test, but this was not observed repeatedly so from this data it is not valid to draw the conclusion that the observed crystal deformation was a result of electrokinetics. According to EDX results, there does seem to be a tendency for chromium and the high-contrast, titanium-rich deposits to exist together. Weight percentages of chromium are significantly higher when it is found within the titanium-rich particles that were repeatedly observed within the Cr, Ni and Cd test. This suggests that the titanium-rich particles have more surface charge associated with them.

### 4.2. X-ray diffraction results

The initial sample and the samples from the five sections of each EK test were X-rayed and the diffraction patterns for the three EK tests were obtained. The 0 0 1 and 0 0 2 kaolinite peak positions and heights for each sample were determined and the changes in peak position after EK were assessed. Using the soil pH values from Reddy et al. [2], the changes in peak height with increasing soil pH were also examined.

The diffraction pattern for each initial sample was compared to post-EK patterns in Fig. 10. For all three EK tests, there were no significant changes in the position of the 0 0 1 or 0 0 2 kaolinite peaks when the diffraction pattern for the initial sample was compared to each post-EK diffraction pattern. As seen in Fig. 11(a), there were also no significant changes in peak position with distance from the anode. A shift in peak position is directly related to changes in interatomic distance (d-spacing), hence the Bragg equation:

$$n\lambda = 2d\sin\theta \quad (3)$$

where $n$ is an integer, $\lambda$ is the wavelength of the incident X-ray beam, $d$ is the d-spacing (distance between two atomic planes, planes specified by the miller index, i.e. 0 0 1, 0 02) and $\theta$ is the angle of the incident X-ray beam. A significant change in peak position after EK, or with changes in pH could indicate that cations, water or molecules were somehow entering the clay mineral structure and altering interatomic distances. However, all changes in peak position that were observed were subtle and did not appear to be related to pH changes or to the application of electrokinetic potential.

Peak intensity and peak height are related to each other, but peak intensities are given by the Jade program as relative percentages within one diffraction pattern. It is therefore more reasonable to compare peak height (in counts) when comparing one diffraction pattern to another. A plot of peak height with normalized distance from the anode is shown in Fig. 11(b). This plot suggests a decrease in peak height within the first 2 or 3 sections of each test (the low pH region). So peak height was then compared to soil pH initially

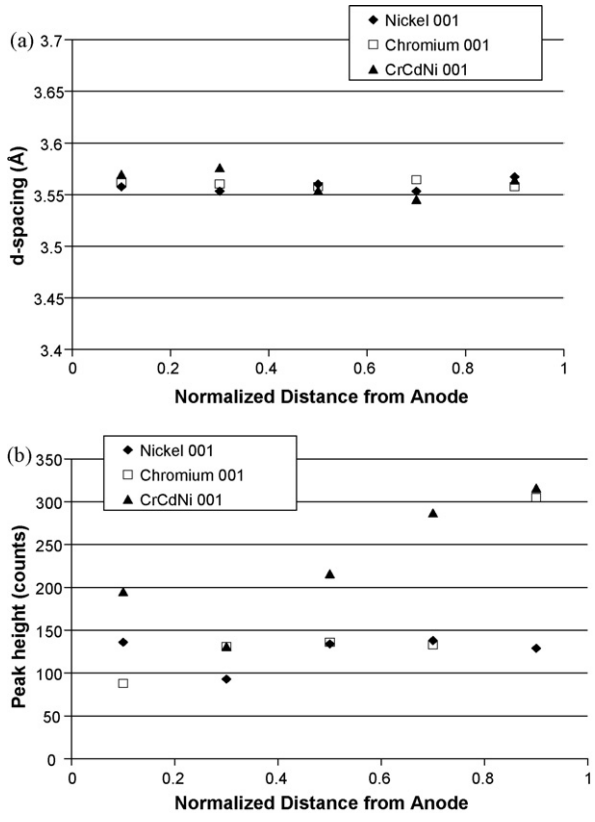


**Fig. 11.** XRD data analysis: (a) A comparison of the values for d-spacing with normalized distance from anode for all five sections of all three tests, (b) A comparison of the values for peak height with normalized distance from anode for all five sections of all three tests.

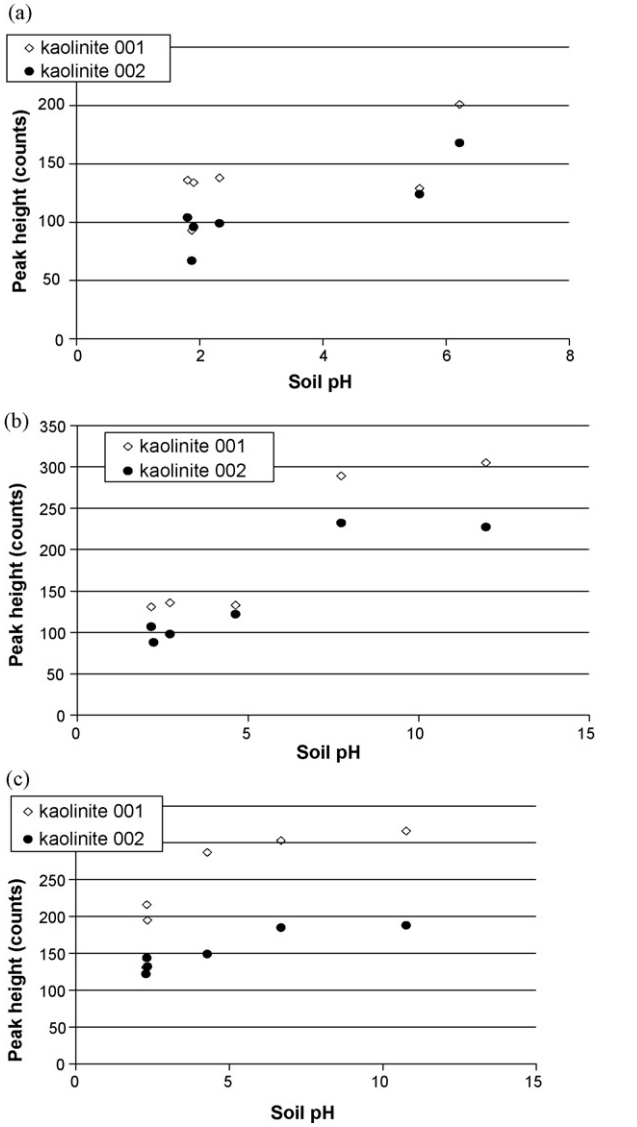


**Fig. 12.** A plot of the values for kaolinite 0 0 1 and 0 0 2 peak heights against soil pH for initial spiked soil, and all five sections of (a) Ni only test, (b) Cr only test, and (c) mixed contaminants (Cr, Ni and Cd) test.

and within the test cell. In all three EK tests, the 001 and 002 kaolinite peaks both show lower heights with lower soil pH (Fig. 12). It is easiest to see the differences in peak height when looking at the chromium test. Peak heights appear significantly lower at pH values below 5. For the nickel test, peak height was lower at pH values below 6 than at values above 6. For the test with multiple metals, the peak height still decreased with decreasing pH but the transition seems more gradual. These results imply that there may have been some dissolution of kaolinite taking place, because if the crystal structure was broken down due to ambient low pH during the EK treatment, there would be fewer reflections to contribute to the diffraction pattern and hence a lower peak intensity. Carol-Webb and Walther [23] and Eykholt [33] reported that kaolinite may dissolve during EK as a result of pH changes within the pore fluid, namely at pH values above 9 and below 4. However, it should be noted that in the results for this study the diffraction patterns only reflect peak height decreases in acidic regions. For the nickel test, a soil pH of 12 did in fact exist in Section 5 but the diffraction pattern for Section 5 did not show a decrease in peak height.

Overall, based on the diffraction patterns, no significant changes in peak position resulted from the electrokinetic remediation alone, or from changes in soil pH, which may be attributed to kaolinite being not expandable clay. The diffraction patterns did show that there was a decrease in peak intensity with decreasing soil pH value, which may represent dissolution of kaolinite minerals during electrokinetic remediation. However past research reflects that kaolinite also has a high propensity for dissolution at a pH above 9 [23], and the diffraction pattern did not reflect any decrease in peak height for Section 5 of the nickel test, which had a soil pH of 12.

## 5. Conclusions

This study investigated the physical distribution of heavy metals in kaolin and the chemical and structural changes in kaolinite minerals that resulted from electrokinetic remediation. TEM and EDX analyses were performed on the soil samples before and after electrokinetic remediation to determine any changes in heavy metal phase or changes in kaolinite platelets. It was concluded that heavy metal contaminant distribution in the soil samples was not observable using TEM and EDX. EDX detected nickel and chromium on some kaolinite particles and titanium-rich, high-contrast particles, but no separate phases containing the added metal contaminants were detected. Small amounts of heavy metal contaminants that were detected by EDX in the absence of a visible phase suggest that ions are adsorbed to kaolinite particle surfaces as a thin coating. There was also no clear correlation between semiquantitative analysis of EDX spectra and measured total metal concentrations, which may be attributed to low heavy metal concentrations and small size of samples used. To detect any structural changes in kaolinite minerals resulting from EK, X-ray diffraction analyses were performed on all kaolin samples. The diffraction patterns showed a decrease in peak height with decreasing soil pH value, which indicates possible dissolution of kaolinite minerals during electrokinetic remediation.

## References


[1] US Environmental Protection Agency, Cleaning up the Nations' Waste Sites: Markets and Technology Trends, EPA 542-R-96-005, Office of Solid Waste and Emergency Response, Washington, DC, 1997.

[2] K.R. Reddy, S. Chinthamreddy, A.Z. Al-Hamdan, Synergistic effects of multiple metal contaminants during electrokinetic remediation, Remediation 11 (2001) 85–109.

[3] K.R. Reddy, C. Chaparro, R.E. Saichek, Iodide-enhanced electrokinetic remediation of mercury-contaminated soils, J. Environ. Eng. 129 (2003) 1137–1148.

[4] K.R. Reddy, S. Chinthamreddy, Sequentially enhanced electrokinetic remediation of heavy metals in low buffering clayey soils, J. Geotech. Geoenviron. Eng. 129 (2003) 263–277.

[5] K.R. Reddy, S. Danda, R.E. Saichek, Complicated factors of using ethylenediamine tetraacetic acid to enhance electrokinetic remediation of multiple heavy metals in clayey soils, J. Environ. Eng. 130 (2004) 1357–1366.

[6] A.Z. Al-Hamdan, K.R. Reddy, Transient behavior of heavy metals in soils during electrokinetic remediation, Chemosphere 71 (2008) 860–871.

[7] J.L. Chen, S.R. Al-Abed, L.T. Bryndzia, L. Murdoch, Cation transport and partitioning during a field test of electroosmosis, Water Resour. Res. 35 (1999) 3841–3851.

[8] T. Lemaire, C. Moyne, D. Stemmelen, Modelling of electro-osmosis in clayey materials including pH effects, Phys. Chem. Earth 32 (2007) 441–452.

[9] R.S. Li, L.Y. Li, Enhancement of electrokinetic extraction from lead spiked soils, J. Environ. Eng. 126 (2000) 849–857.

[10] A. Altin, M. Degirmenci, Lead(II) removal from natural soils by enhanced electrokinetic remediation, Sci. Total Environ. 337 (2005) 1–10.

[11] D. Zhou, C. Deng, L. Cang, A.N. Alshawabkeh, Electrokinetic remediation of a Cu–Zn contaminated red soil by controlling the voltage and conditioning catholyte pH, Chemosphere 61 (2005) 519–527.

[12] D. Rai, L.E. Eary, Zachara environmental chemistry of chromium, Sci. Total Environ. 86 (1989) 15–23.

[13] K.R. Reddy, U.S. Parupudi, S.N. Devulapalli, C.Y. Xu, Effects of soil composition on the removal of chromium by electrokinetics, J. Hazard. Mater. 55 (1997) 135–158.

[14] A. Sawada, K. Mori, S. Tanaka, M. Fukushima, K. Tatsumi, Removal of Cr(VI) from contaminated soil by electrokinetic remediation, Waste Manag. 24 (2004) 483–490.

[15] A. Li, K.A. Cheung, K.R. Reddy, Cosolvent-enhanced electrokinetic remediation of oils contaminated with phenanthrene, J. Environ. Eng. 126 (2000) 527–533.

[16] S. Yuan, M. Tian, X. Lu, Electrokinetic movement of hexachlorobenzene in clayed soils enhanced by Tween 80 and β-cyclodextrin, J. Hazard. Mater. 137 (2006) 1218–1225.

[17] K. Maturi, K.R. Reddy, Simultaneous removal of organic compounds and heavy metals from soils by electrokinetic remediation with a modified cyclodextrin, Chemosphere 63 (2006) 1022–1031.

[18] K. Maturi, K.R. Reddy, Cosolvent-enhanced desorption and transport of organic and metal contaminants in soils during electrokinetic remediation, Water Air Soil Pollut. 189 (2008) 199–211.

[19] S. Chinthamreddy, K.R. Reddy, Oxidation and mobility of trivalent chromium in manganese-enriched clays during electrokinetic remediation, J. Soil Contam. 8 (1999) 197–216.

[20] P. Isosaari, R. Piskonen, P. Ojala, S. Voipio, K. Eilola, E. Lehmus, M. Itävaara, Integration of electrokinetics and chemical oxidation for the remediation of creosote-contaminated clay, J. Hazard. Mater. 144 (2007) 538–548.

[21] K.R. Reddy, S. Chinthamreddy, Electrokinetic remediation of heavy metal contaminated soils under reducing environments, Waste Manag. 19 (1999) 269–282.

[22] A.T. Yeung, C. Hsu, R.M. Menon, Physicochemical soil-contaminant interactions during electrokinetic extraction, J. Hazard. Mater. 55 (1997) 221–237.

[23] S.A. Carroll-Webb, J.V. Walther, A surface complex reaction model for the pH-dependence of corundum and kaolinite dissolution rates, Geochim. Cosmochim. Acta 52 (1988) 2609–2623.

[24] L. Yang, C.I. Steefel, Kaolinite dissolution and precipitation kinetics at 22 °C and pH 4, Geochim. Cosmochim. Acta 72 (2008) 99–116.

[25] Y. Lan, C. Li, J. Mao, J. Sun, Influence of clay minerals on the reduction of $Cr^{6+}$ by citric acid, Chemosphere 71 (2008) 781–787.

[26] A.Z. Al-Hamdan, Speciation, distribution and mobility of heavy metals in soils during electrokinetic remediation, Ph.D. Thesis, University of Illinois at Chicago, Chicago, IL, 2002.

[27] H.H. Murray, Kaolin minerals: their genesis and occurrences, Rev. Mineral. 19 (1988) 67–87.

[28] A.Z. Al-Hamdan, K.R. Reddy, Geochemical reconnaissance of heavy metals in kaolin after electrokinetic remediation, J. Environ. Sci. Health A41 (2006) 17–33.

[29] A.Z. Al-Hamdan, K.R. Reddy, Geochemical assessment of metal transport in glacial till during electrokinetic remediation, Environ. Monit. Assess. 139 (2008) 137–149.

[30] A.Z. Al-Hamdan, K.R. Reddy, Electrokinetic remediation modeling incorporating geochemical effects, J. Geotech. Geoenviron. Eng. 134 (2008) 91–105.

[31] W.D. Schecher, W.D. McAvoy, MINEQL+: A Chemical Equilibrium Program for Personal Computer, User's Manual, Environmental Research Software, Hallowell, ME, 1994.

[32] N. Roach, Mineral structure and particle morphology of kaolin subjected to electrokinetic remediation, M.S. Thesis, University of Illinois at Chicago, Chicago, IL, 2002.

[33] G.R. Eykholt, Driving and complicating features of the electrokinetic treatment of contaminated soils, Ph.D. Thesis, The University of Texas at Austin, 1992.

[34] S. Chinthamreddy, Geochemical characterization and enhanced mobilization of heavy metals during electrokinetic remediation of soils. Ph.D. Thesis, University of Illinois at Chicago, Chicago, IL, 1999.